Visualization of High-Dimensional Combinatorial Catalysis Data

Changwon Suh,[†,||] Simone C. Sieg,[‡,||,⊥] Matthew J. Heying,[§,||] James H. Oliver,[§,||] Wilhelm F. Maier,[‡,||] and Krishna Rajan*[,†,||]

Department of Materials Science and Engineering, Iowa State University, Ames, IA, Technische Chemie, Saarland University, Saarbrücken, Germany, Virtual Reality Applications Center, Iowa State University, Ames, IA, and NSF International Materials Institute: Combinatorial Sciences and Materials Informatics Collaboratory (CoSMIC-IMI)

Received November 25, 2008

The role of various techniques for visualization of high-dimensional data is demonstrated in the context of combinatorial high-throughput experimentation (HTE). Applying visualization tools, we identify which constituents of catalysts are associated with final products in a huge combinatorially generated data set of heterogeneous catalysts, and catalytic activity regions are identified with respect to pentanary composition spreads of catalysts. A radial visualization scheme directly visualizes pentanary composition spreads in two-dimensional (2D) space and catalytic activity of a final product by combining high-throughput results from five slate libraries. A glyph plot provides many possibilities for visualizing high-dimensional data with interactive tools. For catalyst discovery and lead optimization, this work demonstrates how large multidimensional catalysis data sets are visualized in terms of quantitative composition activity relationships (QCAR) to effectively identify the relevant key role of compositions (i.e., lead compositions) of catalysts.

Introduction

Combinatorial approaches in materials design and synthesis have been increasingly used for the systematical finding of new materials, but data analysis generated combinatorial approaches are very limited due to the huge amount of multivariate characteristics of the data sets. This disparity between high-throughput synthesis and low-throughput data interpretation is still problematic in combinatorial materials science. To resolve this issue, high-throughput data for material discovery can be interpreted utilizing visualization techniques describing complex hidden relationships, patterns, QCAR, or outliers in the data. The importance of visualization in science cannot be overemphasized because it provides a direct method to depict scientific data to better understand physical meanings. Visualization extends beyond displaying data to include the transformation of huge interrelated multivariate data from combinatorial libraries into information space.[1]

However, it is not a trivial task to find informative patterns by representing relative contributions in few dimensions because of the multi (or high)-dimensional nature of high-throughput data sets. An example of a direct visualization method is the traditional Cartesian coordinate mapping of data in *x*- and *y*- or *x*-, *y*-, and *z*-space using axes that are orthogonal to each other. To overcome the limitations of Cartesian coordinates in displaying multidimensional data, a scatterplot matrix consisting of possible arrays of bivariate plots has been used, although the scatterplot matrix still must be considered from many different projections. An example of an indirect data mapping method to handle high-dimensional data is data mining techniques for dimensionality reduction such as principal component analysis (PCA). Interpreting complex data with PCA, however, is cumbersome because of the difficulty in transforming the data in principle component space back into the experimental framework. The principal components explain data trends of observed random variables in terms of a reduced number of unobserved variables, which are a linear combination of the original variables that have been transformed onto a new coordinate system based on the order of variance in the data. Therefore, it is sometimes more convenient for interpretation to use alternative ways of visualization for multidimensional data sets without dimensionality reduction.

Information visualizations of multidimensional data sets have been recognized as very crucial to depicting multiple gene expressions in a field of biotechnology or genetics.

Scheme 1. Detected Products of Propene Oxidation at 350 °C Using 1001 Catalysts Consisting of Mixed Metal Oxides

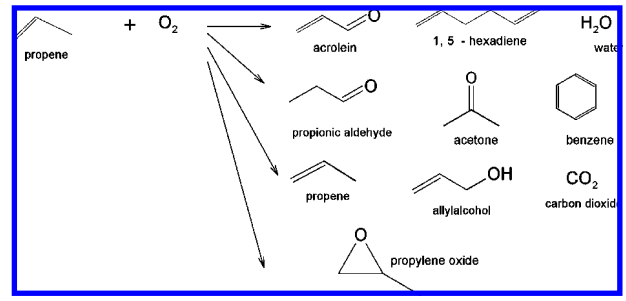

* To whom correspondence should be addressed. Phone: +1 515 294 2670. Fax: +1 515 294 5444. E-mail: krajan@isatate.edu.
† Department of Materials Science and Engineering, Iowa State University.
|| CoSMIC-IMI.
‡ Saarland University.
⊥ Current Address: hte Aktiengesellschaft, Kurpfalzring, Heidelberg, Germany.
§ Virtual Reality Applications Center, Iowa State University.

10.1021/cc800194j CCC: $40.75
Published on Web 03/19/2009

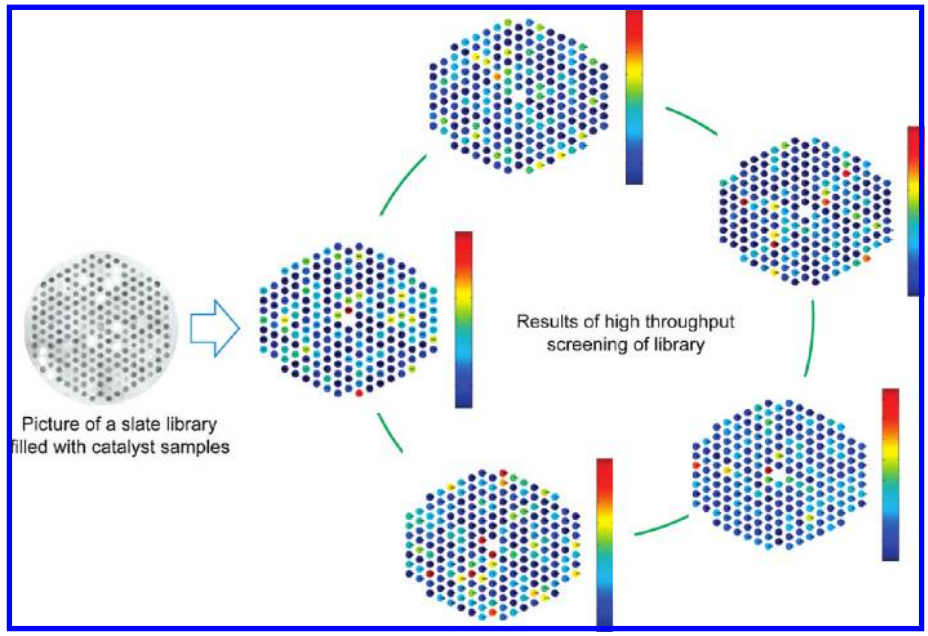

Figure 1. Slate library and results of high-throughput screening of the 5 libraries. Two hundred wells on each slate library are filled with catalyst samples; 3 are filled with reference samples (Hopcalite), and 3 wells are left empty for additional reference. Five different slate plates were used for full screening of a complete pentanary composition spread (i.e., 1001 catalysts). The color codes the size of the detected GC signal for acrolein. Best catalysts (samples) appear in (dark) red.

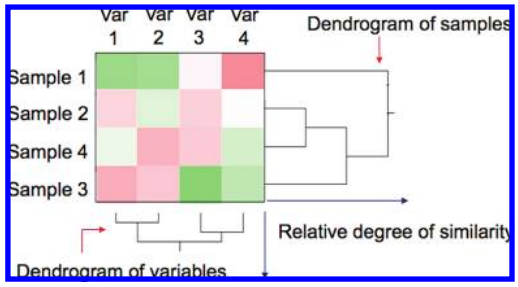

Figure 2. An intuitive example of a heat map. A heat map displays the data table as grids of rectangular shapes and provides the associations of samples and variables (properties). On the basis of the color codes changing from green to white to red in the figure, sample 1 has a high value of property 4 (Var 4), while sample 3 has a low value of Var 3. Heat maps usually include hierarchical clusters of properties and instances using dendrograms. While samples 2 and 4 are similarly associated with respect to the four variables, variables 1 and 2 have similar behaviors for the given four samples.

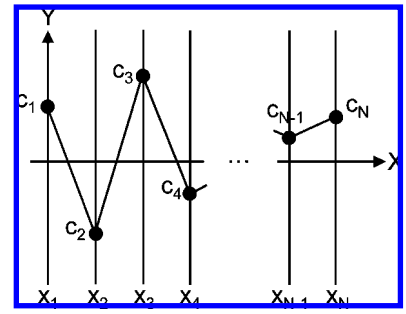

Figure 3. An *N*-dimensional data tuple in parallel coordinates. Each vertical line is an axis equivalent to each dimension (variable), while polygonal lines connect each axis along corresponding dimensional values (c_1, c_2,..., c_N), of each sample.[13] Unlike heat maps, parallel coordinates capture associations of variables instead of samples by creating polygonal lines through variables.

There are some pioneering works for visualization of high-dimensional or combinatorially derived data in chemistry;[2−5] however, visualization of materials science data generated from a combinatorial approach is still in the early stages despite combinatorial approaches with high-throughput synthesis in materials design and synthesis developing quickly. As a test bed in this paper, we provide a demonstration of different sophisticated visualization strategies of high-dimensional catalysis data obtained through combinatorial experiments to visualize composition-activity relationships, which are highly desirable to understand heterogeneous catalysts. The purpose of this study is not to develop new catalysts but to demonstrate how to explain and extract composition−activity relationships in the context of catalysts with different visualization methods, such as heat maps and parallel coordinates, in combinatorially derived data sets. Using a radial visualization technique, composition−catalytic activity relationships are also visualized with respect to combinatorial arrays in a slate library used for data generation.

Experimental Section

All data considered here have been obtained by high-throughput screening of a complete pentanary composition spread consisting of five chemical elements (Cr, Mn, Co, Te, and Ni) as oxides in a 10 mol % wide variation of compositions (more precisely, the final catalysts consist of mixed metal oxides in predefined ratios). Each sample has the following composition.

$$Cr_aMn_bCo_cTe_dNi_e \text{ with } a + b + c + d + e = 1 \text{ and } a, b, c, d, e \text{ in } [0, 1 \text{ mol } \%]$$

A variation of five elements in this way yields 1001 samples, including binary, ternary, and quaternary samples. In addition, the pure metal oxides of Cr, Mn, Co, Te, and Ni have been considered as part of the search space. The catalysts, appearing in the shape of powders, have been

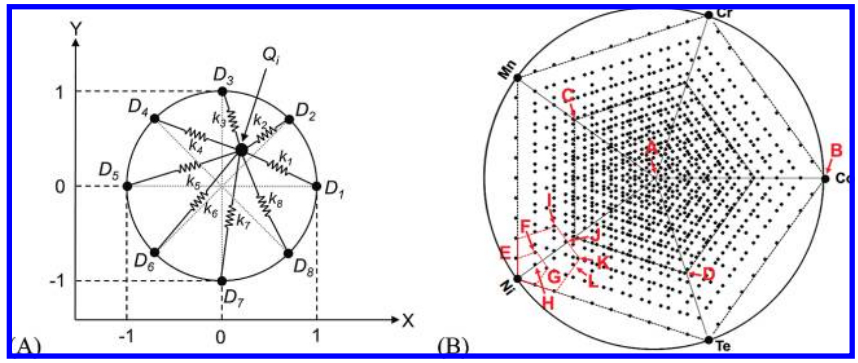

Figure 4. (A) Radial visualization mapping of an 8D space onto a 2D space. 8D space generates 8 DAs and a data point Q_i is connected to each DA by eight springs like a trampoline. (B) An example of radial visualization for a composition spread of pentanaries with 10% wise compositional increments. Some interesting points are marked for convenience. Points E, F, G, and H are for 90% of Ni while points I, J, K, and L are for 80% of Ni. With the order of (Mn, Ni, Te, Co, Cr), each point is assigned as follows: point A = (0.2,0.2,0.2,0.2,0.2), B = (0,0,0,1,0), C = (0.4,0.3,0,0,0.3), D = (0,0.3,0.4,0.3,0), E = (0.1,0.9,0,0,0), F = (0,0.9,0,0,0.1), G = (0,0.9,0,0.1,0), H = (0.1,0.8,0.1,0,0), I = (0,0.8,0,0,0.2), J = (0,0.8,0,0.1,0.1), K = (0,0.8,0,0.2,0), L = (0,0.7,0.2,0,0.1). Color-coding of the points provides functional information.

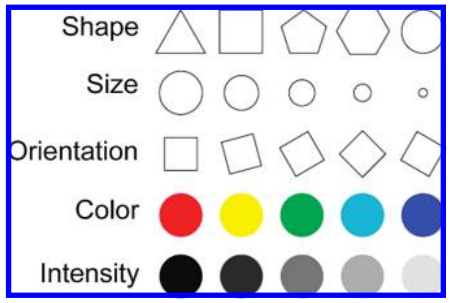

Figure 5. Commonly used glyph attributes for high speed preattentive processing.

synthesized using a high-throughput synthesis route, following an acid-catalyzed sol−gel process. The following precursors have been used: Cr(III)-propionate, Co(II)-propionate, Ni(II)-propionate, Mn(II)-propionate, and telluric acid. All solid metal precursors were dissolved in methanol in a concentration of 0.5 mol/L. The precursor solutions were mixed by means of a dispensing robot in appropriate ratios to give the final desired composition. Additionally, propionic acid (PA), the complexing agent 4-hydroxyl-4-methyl-2-pentanone (CA) and methanol have been dosed and added by the robot. The molar ratios of the additives relative to the sum of the base ions (1) was 0.3 PA/6 CA/47,5 MeOH. After the gelation procedure, the samples have been calcined at 400 °C to remove remaining solvent. Finally, the catalyst samples have been screened for catalytic activity in the oxidation of propene at 350 °C as a model reaction in a high-throughput test reactor system. Special attention has been paid to the problem of comparability of the many catalyst samples generated. All syntheses have been obtained by a single sol−gel procedure highly tolerant to all compositional changes applied. Gelation time, calcination, and treatments have been carried out in parallel, so highly amorphous porous mixed oxides of comparable microstructure are generated. The detailed setup of the test reactor has been already described in refs 6−8, while a more detailed description of the catalyst preparation can be found in the Ph.D. thesis of one of the authors.[9] Scheme 1 summarizes the chemical reaction studied and also gives an overview on all detected products that have been monitored for each sample by gas-chromatography (GC) measurements. The data we are dealing with in this study exclusively focus on the formation of acrolein among all products. Acrolein was chosen because of its high abundance in the products and its importance as a base chemical. For the screening itself, the 1001 samples have been randomly split and transferred to five identical slate libraries that contain 206 wells to hold the catalyst powders (Figure 1).

The high-throughput screening approach chosen here generates large amounts of experimental data that need to be analyzed and interpreted. In this study, we demonstrate the application of visualization techniques to this combinatorial catalyst data set as a case study. Figure 1 depicts the raw data from high-throughput screening. Each slate plate is transferred to the reactor system such that each well serves as a small reaction chamber where the gaseous reaction takes place. A mixture of propene and synthetic air is passed over the library at 350 °C. After a defined reaction time, the product gas mixture leaving the reaction chamber is analyzed by GC measurements for the products listed in Scheme 1. The color-coded GC signals for the selected acrolein are given in Figure 1. Red indicates a large GC signal, while blue samples represent only little acrolein in the product gas mixture. The aim of these experiments has been to indentify samples that lend themselves to the selective oxidation of propene to acrolein as well as to identify correlations between the chemical composition of the materials and their catalytic performance. Clearly, this visualization identifies the relative activity of all samples on the library, but neither identity of the samples nor correlations of activity, selectivity, and chemical composition are visible.

Methods

Various visualization techniques have been developed for visualizing high-dimensional data. The three popular schemes used in this paper are heat maps, parallel coordinates, and radial visualizations. It is demonstrated how these visualizations help to identify composition-activity relationships from the measured catalytic activities to four products and the composition spreads of different constituents of catalysts. All of these visualization schemes map the original high-dimensional feature space onto 2D space without any feature

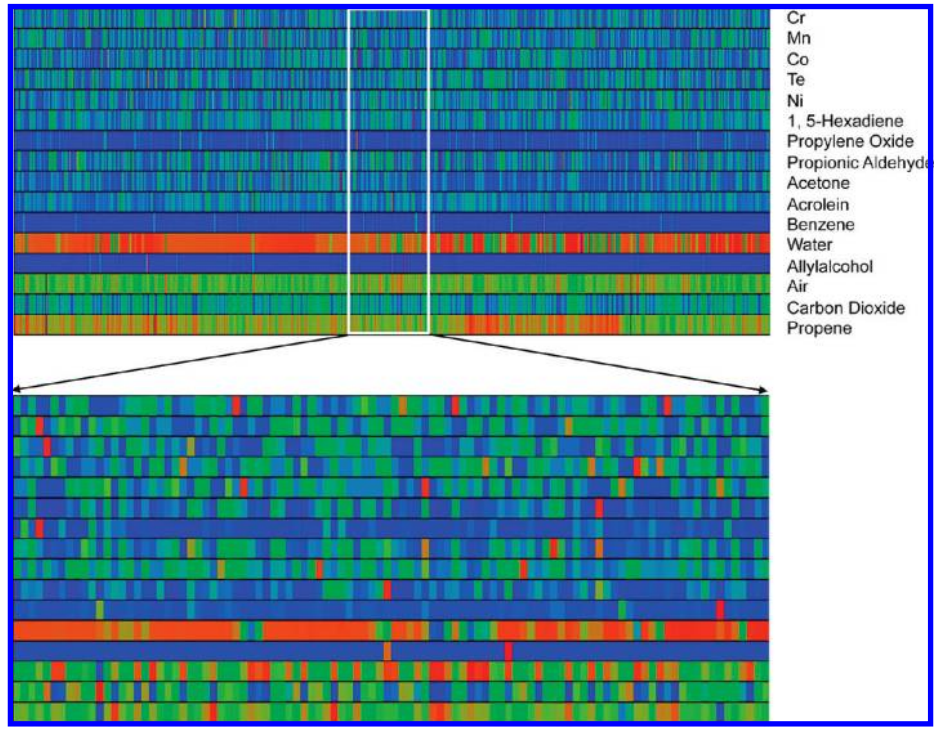

Figure 6. Representation of 1001 catalyst samples by a cell plot. The color corresponds to the composition and activity of acrolein of the sample. Color codes change from blue (low value) to green to red (high value).

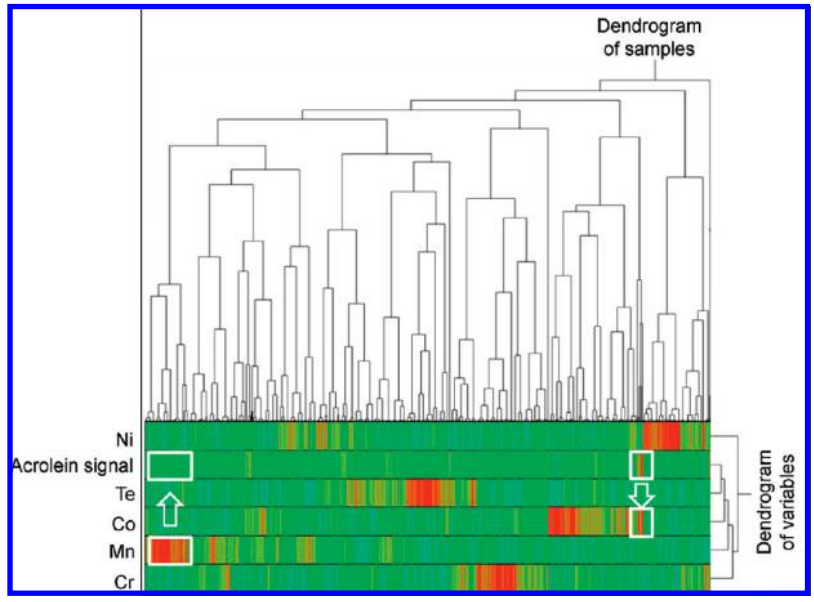

Figure 7. A heat map for visualization of 1001 catalysts in terms of a pentanary composition spread and catalytic activity for acrolein formation. Hierarchical clustering analysis in this figure is based on the average-linkage algorithm and two-way clustering (i.e., clustering for catalysts as well as variables) was performed. The figure was color coded by "blue to green to red" scheme. Thus, higher values appear in red grids while blue codes for lower values. The high activity region for acrolein (white box marked on the right) is related to larger Cocontents of the mixed oxides. Large amounts of Mn (white box marked on the left) lead to low activity of acrolein. This argument can be applied for composition activity relationships for other elements as well. Note that the order of the rows and columns were determined by cluster analysis.

reductions such as from PCA. Therefore, interpretation of data with high-dimensional visualization techniques is typically more transparent and better understandable than feature reduction techniques. High-dimensional visualization techniques also help to easily identify trends in properties including clusters or outliers of the data set. In this paper, visualization tools are adapted to visualize compositions for five factors (constituent elements of catalysts) and one response (activity of acrolein) of 1001 catalyst samples in 2D space.

Heat Maps. Visualization by heat maps is a direct mapping method for depicting raw data. In heat maps, an intersection of a pair of rows and columns creates a grid associated with a pair of sample and property (Figure 2).

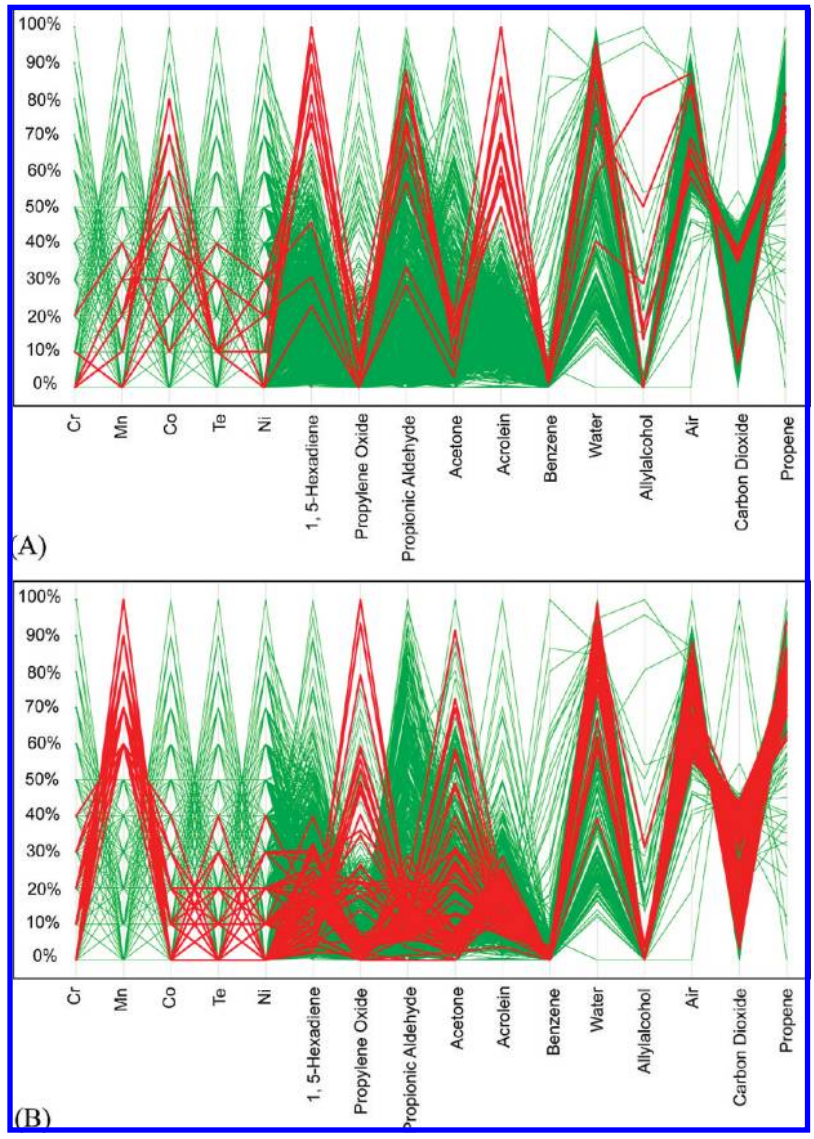

Figure 8. (A) Parallel coordinates brushed in red for high activities (upper 50%) of acrolein. (B) Parallel coordinates brushed in red for high contents (upper 60%) of Mn. Associations of factors and a response are visualized by brushing technique in parallel coordinates.

The color of each rectangle corresponds to a value in the samples. Therefore, it can be considered as a color-coded data table. The order of the rows and columns is determined by cluster analysis. By combining direct mapping of data points onto a grid with dendrograms from cluster analysis, heat maps are often used for visualizing microarray data in genetics to quickly identify critical regions and hidden interrelationships between samples or variables.

Parallel Coordinates. Parallel coordinate systems map an N-dimensional data space (R^N) onto the 2D display by drawing N equally spaced axes parallel to one of the display axes.[10] As shown in Figure 3, a point of (c_1, c_2,..., c_N) in N-dimensional space is shown by polygonal lines that intersect each x-axis. In principle, parallel coordinates are feasible to visualize ultra high-dimensional data. However, because a large set of polygonal lines are generally generated by huge amounts of samples, an interaction technique is indispensable to avoid a data cluttering problem in parallel coordinate plots. Basic interactions with parallel coordinates occur through the brushing technique. By selecting interesting polygonal lines, existing correlations between axes can be easily identified for brushed (highlighted) polygonal sets. Other useful interaction techniques for parallel coordinates are explained in the literature.[11,12]

Radial Visualization. To map out a set of multidimensional points onto 2D space, radial visualization uses the concept of Hooke's law, which describes the spring's restoring force as $F(x) = -kd$, where k is the spring constant and d is the displacement. The shape of radial visualization is similar to a trampoline. When m variables in a data set need to be visualized, m points in radial visualization are arranged to be equally spaced around the circumference of the circle having a radius of 1 (Figure 4A). Each point is called a dimensional anchor (DA, D_1 to D_m). Ends of these DAs are fixed at one point connected with m springs in a circle. The spring constant k_i is the scaled data value in each dimension.

The location of each data point is assigned at the equilibrium position where the sum of spring forces is zero. This point $Q_i = (x_i,y_i)^T$ in Figure 4A represents the projection in 2D space of the point in m-dimensional space (i.e., $R^m \rightarrow R^2$). If a data set consists of m variables, radial visualization

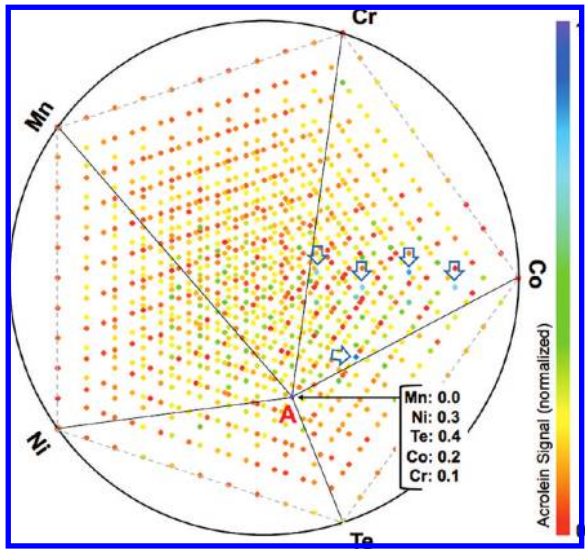

Figure 9. 2D data visualization of the pentanary composition spreads in radial visualization. The color code corresponds to the activity values screened for acrolein. While point A is the point of highest activity for acrolein, blue arrows are also high activity points for acrolein.

creates an *m*-sided polygon. Pentanary compositions create the shape of a pentagon in radial visualization and each vertex represents a single constituent element (Figure 4B). Some features of radial visualization are described in the literature.[1,14−16]

Glyph Plot. A glyph plot is a technique to visualize high-dimensional multivariate data in 2D or 3D space. In a glyph plot, graphical objects (glyphs) are placed at the explicit or implicit spatial coordinates of each data point in the data set. The type of glyph used depends on the nature of the data. For vector data, arrows are typically used to visualize orientation as well as magnitude. For scalar data, geometric primitives such as spheres or cubes are often used, but complex shapes can also be used to visualize high-dimensional data sets. The nonspatial data contained at each data point is mapped to the graphical attributes of the glyph with the goal of exploiting the viewer's preattentive processing that quickly enables them to identify boundaries, clusters, spatial correlations, and outliers. Common glyph graphical attributes include shape, size, color, intensity, orientation, flicker, motion, and texture (Figure 5).[17]

Glyph plots conceptually can visualize high-dimensional data utilizing many possible combinations of glyph attributes. For applications of glyph plots for catalysis data (here from binary to quaternary mixed oxides) in this study, we first construct a tetrahedron for composition spreads so that unaries (pure elements) sit on the vertices, binaries on the edges, and ternaries on the faces of a tetrahedron.[18] It should be noted that composition spreads of pentanary systems are not simply possible to visualize mainly because of the dimensional limit of creating equally important composition gradients of each of the five elements, while some strategies to create high-dimensional gradient arrays in combinatorial experimentation were already devised.[18] In a constructed tetrahedron, spheres as a shape are used to represent catalytic activities, while activities of specific products are assigned by color, size, and intensity of the spheres.

Results and Discussion

As shown in Scheme 1, the detected products of propene oxidation at 350 °C using mixed metal oxide catalysts (from all binaries to pentanaries) include acrolein, 1,5-hexadiene, propionic aldehyde, and others. Prior to visualization, the data are generally pretreated to have the same unit variance for all variables. For the examples of visualization in this paper, local normalization was used. Since five compositions are already designed to change from 0 to 1, a data column of activity of acrolein was additionally scaled from its maximum and minimum to between 0 and 1. In Figure 6, the resulting associations between composition and activity are visualized by a cell plot (i.e., heat map without dendrogram). Since such a cell plot does not include results of cluster analysis, the order of the rows and columns is not changed by a dendrogram, and therefore, Figure 6 is an exact visualized version of a color-coded catalysis data table. Although clusters from huge samples in a cell plot are problematic for the selection of interesting data points, this representation of the data allows a quick visual inspection of the performance of the catalysts.

Unlike a cell plot, a heat map as shown in Figure 7 is designed to provide information on the association of variables (or samples) while maintaining the concepts of a cell plot. This is accomplished by including a dendrogram of variables (five compositions and one activity) and samples (catalysts) from cluster analysis. Since we focus on the formation of acrolein in this study, five factors (compositions) and one response (activity of acrolein) were simply visualized in Figure 7. From the dendrogram of variables in the heat map of Figure 7, a correlation between the activity of acrolein and the compositions of each constituent element of catalysts can be identified. For example, activity of acrolein is related to compositions of elements in the decreasing order of significance, Te > Co > Mn > Cr > Ni. In addition to that, QCAR of interesting regions can also be directly screened and uncovered by visual inspection from the cell plot in a heat map of Figure 7. For example, the composition of Mn is inversely related to the activity of acrolein (as marked with white boxes shown with an up-arrow, where the red and the green shades signifying inverse relationship) and regarding the contents of Co, a high activity region for acrolein is matched with higher concentrations of Co than any other element (shown as white boxes with a down-arrow, where the red shade of acrolein matches with that of Co, signifying a direct relationship).

Parallel coordinates are shown with brushed red lines representing high activity regions in the upper 50% of acrolein and high contents of Mn (upper 60%) in Figure 8A and B, respectively. Activity values of the products have been scaled according to the highest result, that is, the best catalyst for acrolein is set to 100% acrolein signal. For example, acrolein is formed together with propionic aldehyde, 1,5-hexadiene, or water, while acetone and propylene oxide counteract acrolein formation as shown in Figure 8A. High contents of Co lead to a higher activity for acrolein. The

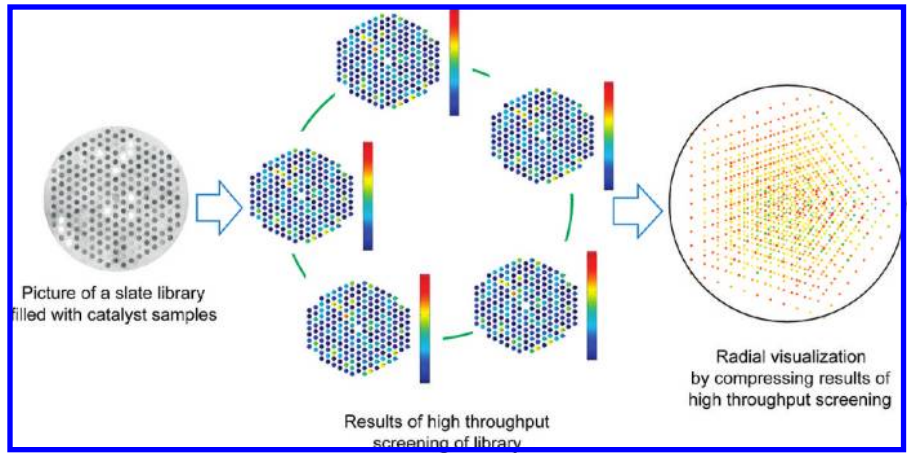

Figure 10. A schematic of the connection between HTE and visualization. For an ideal case, the slate library is fabricated having the same shape as pentanary composition spreads in radial visualization to directly link HTE library with visualization.

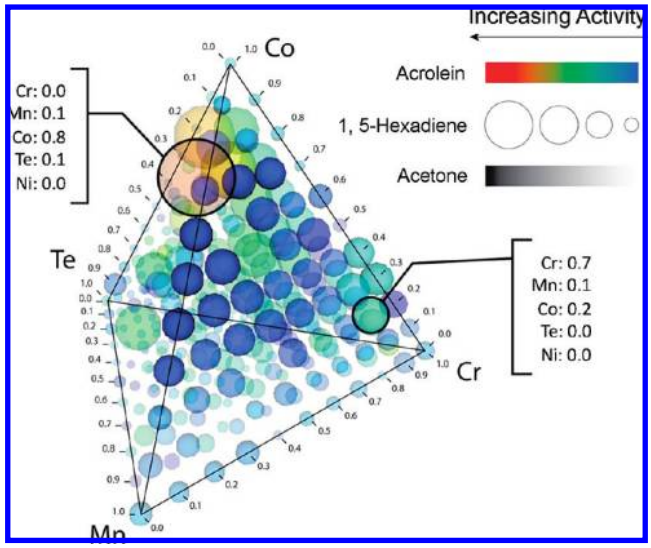

Figure 11. 3D glyph plot of catalyst data. Four elements (Cr, Mn, Co, and Te) are plotted on a 3D quaternary mixtures plot, while three activities are mapped to three graphical attributes of a sphere glyph: color is mapped to activities for acrolein, size is mapped to activities for 1, 5-hexadiene, and intensity is mapped to activities for acetone. The intensity of the glyphs is adjusted on the left plot to accentuate the levels of acetone.

Ⓦ An interactive module for the figure is available as a web-enhanced object and a description of the module is available as Supporting Information.

inverse relationship between contents of Cr and activity for acrolein is quite notable. Although these effects can be confirmed in a heat map (Figure 7), parallel coordinates also provide convenient ways for feature tracking based on the levels of catalytic activities for acrolein to identify composition-activity relationships. Figure 8B is a result after the point of view was changed from activity for acrolein to contents of each constituent element of catalysts. To this end, for instance, the upper 60% of Mn was brushed with red colors and it is obvious that samples having more than 60% of Mn only yielded low acrolein signals, while the formation of propylene oxide and acetone are favored.

While 2D visualization of high-dimensional catalysis data has only been considered so far, it is equally important to include in the visualization scheme the shape of the real experimental design. It is invaluable to combine a composition library with high-dimensional features of catalysis data because it gives us more chances for lead optimization of catalysts by mimicking the experimental setup as much as possible. Figure 9 illustrates the pentanary composition spreads of 1001 catalyst samples in a radial visualization scheme. The color indicates the acrolein signal measured by GC measurements. Because of the regular sampling of the composition space using 10% increment for five elements, the obtained pattern in radial visualization appears as an equilateral pentagon.

The visualization of the pentanary composition spread in this representation allows an immediate investigation of data trends and correlations. For example, point A in Figure 9 is the highest activity point of acrolein. From data distribution for high activity regions with blue arrows in Figure 9, it is identified that Co plays a more important role for the studied reaction while contents of Mn are not very active for acrolein formation. These results are confirmed by parallel coordinates (Figure 8). Figure 10 is a schematic to explain that radial visualization of composition spreads can depict the shape of the library. Although the composition library in the field of HTE catalyst should be adaptable for all aspects of experiments, if the HTE library is designed with a pentagon shape it can be easily visualized and analyzed through radial visualization to track data trends in terms of catalytic activities.

A 3D glyph plot of the catalyst data is shown in Figure 11. The chemical composition of four elements is mapped to a 3D quaternary mixtures plot forming a tetrahedron. Each data point located at one of the four vertices of the tetrahedron represents a pure element, while interior data points represent a mixture of the four elements. For this data set, the composition spread was developed in a 10 mol % wide variation. For each data point, a sphere glyph is placed at the point's transformed x, y, z spatial coordinates. For the glyph plot shown in Figure 11, three activities have been mapped to three graphical attributes of the sphere: the color is mapped to acrolein (blue for low- and red for high activities), the size is mapped to 1,5-hexadiene, and the intensity is mapped to acetone. The glyph plots were created with a custom-built software tool that allows users to interactively modify mappings and axes of the glyph plot.

For example, modifying the intensity mapping from high to low quickly shows qualitatively a strong correlation between low acrolein levels, medium 1,5-hexadiene levels, and high acetone levels in a particular chemical space region.

Conclusions

In this paper, we have shown how complex high-dimensional materials data can be visualized in low-dimensional space. With catalysis data sets generated from HTE, we also demonstrated how to find composition−activity relationships from huge data sets through information visualization. Each different visualization scheme has cons and pros. A heat map provides association between factors and responses along with color-coded data table. While parallel coordinates allow us to visualize data trends by brushing techniques, radial visualization is useful to visualize complex composition spreads in HTE. Therefore, one can take advantage of visualization as a tool to accelerate the interpretation of complex data sets by combining different perspectives of data representation. In high-throughput screening setups, much analysis data is produced within a rather short time period such that the effective data analysis by the researchers is of great importance. Low-dimensional visualizations are mainly demonstrated in this work. For further work, identification of interesting data points across each visualization scheme will be applied for high-dimensional data in detail based on the authors' previous work with the brushing technique.[19] In addition, high-dimensional glyph visualization of pentanary systems in catalyst data will be also considered in detail.

Acknowledgment. We thank the "National Science Foundation: International Materials Institute program—Combinatorial Sciences and Materials Informatics Collaboratory (CoSMIC-IMI)" Grant DMR-08-33853, for support.

Supporting Information Available. PDF explaining the interactive module. This material is available free of charge via the Internet at http://pubs.acs.org.

References and Notes

(1) Gee, A. G.; Yu, M.; Li, H.; Grinstein, G. G. *Dynamical and Interactive Dimensional Anchors for Spring-Based Visualizations*; Technical Report 2005-012; Computer Science, University of Massachusetts: Lowell, MA, 2005.
(2) Vander Heyden, Y.; Pravdova, V.; Questier, F.; Tallieu, L.; Scott, A.; Massart, D. L. *Anal. Chim. Acta* **2002**, *458*, 397–415.
(3) Frantzen, A.; Sanders, D.; Scheidtmann, J.; Simon, U.; Maier, W. F. *QSAR Comb. Sci.* **2005**, *24*, 22–28.
(4) Chevrier, V.; Dahn, J. R. *Meas. Sci. Technol.* **2006**, *17*, 1399–1404.
(5) Mentges, M.; Sieg, S. C.; Schröter, C.; Frantzen, A.; Maier, W. F. *QSAR Comb.Sci.* **2008**, *27*, 187–197.
(6) Weiss, P. A.; Saalfrank, J. W.; Scheidtmann, J.; Schmidt, H. W.; Maier, W. F. High-throughput gas chromatography and mass spectrometry for heterogeneous catalysis: screening of catalytic activities and selectivities. In *High-Throughput Analysis: A Tool for Combinatorial Materials Science*, 1st ed.; Potyrailo, R. A., Amis, E. J., Eds.; Kluwer: New York, 2003; pp 125−153.
(7) Urschey, J.; Weiss, P.-A. W.; Scheidtmann, J.; Richter, R.; Maier, W. F. *Solid State Sci.* **2003**, *5*, 909–916.
(8) Kim, D. K.; Maier, W. F. *J. Catal.* **2006**, *238*, 142–152.
(9) Sieg, S. C. *Modelling Quantitative Composition Activity Relationships (QCARs) for Heterogeneous Catalysts by Kriging and a Multilevel B-Splines Approach*; Saarland University: Saarbrücken, Germany, 2007.
(10) de Oliveira, M. C. F.; Levkowitz, H. *IEEE Trans Vis. Comput. Gr.* **2003**, *9*, 378–394.
(11) Siirtola, H.; Räihä, K. *Interact. Comput.* **2006**, *18*, 1278–1309.
(12) Kosara, R.; Hauser, H.; Gresh, D. *Proc. Eurograph.* **2003**, 123–137.
(13) Inselberg, A.; Dimsdale, B. *Proc. IEEE Vis. '90* **1990**, 361–378.
(14) Brunsdon, C.; Fotheringham, A. S.; Charlton, M. E. *An Investigation of Methods for Visualising Highly Multivariate Datasets*; Technical Report Series 43; 1998; pp 55−80.
(15) McCarthy, J. F.; Marx, K. A.; Hoffman, P. E.; Gee, A. G.; O'Neil, P.; Ujwal, M. L.; Hotchkiss, J. *Ann. N.Y. Acad. Sci.* 2004, *1020*, 239−262.
(16) Leban, G.; Zupan, B.; Vidmar, G.; Bratko, I. *Data Min. Knowledge Discovery* **2006**, *13*, 119–136.
(17) Healey, C. G.; Booth, K. S.; Enns, J. T. *ACM Trans. Comput.-Hum. Interact.* **1996**, *3*, 107–135.
(18) Cawse, J. N.; Wroczynski, R. Combinatorial Materials Development using Overlapping Gradient Arrays: Designs for Efficient Use of Experimental Resources. In *Experimental Design for Combinatorial and High Throughput Materials Development*; Cawse, J. N., Ed.; John Wiley & Sons, Inc: Hoboken, NJ, 2003; pp 109−127.
(19) Heying, M.; Suh, C.; Rajan, K.; Sieg, S.; Maier, W. F. *Science* **2006**, *313*, 1730–1735.

CC800194J